MBARI Dorado AUV's Scientific Results

Duane Thompson, David Caress, David Clague, Doug Conlin, Julio Harvey, Eric Martin, Jennifer Paduan, Charles Paull, John Ryan, Hans Thomas, Yanwu Zhang
Monterey Bay Aquarium Research Institute
Moss Landing, CA, United States of America

Abstract—**The Monterey Bay Aquarium Research Institute has been developing Autonomous Underwater Vehicles since 2000. Two sizes currently exist: Dorado class AUVs and Long Range AUVs. This document focuses on recent scientific discoveries made with the Dorado AUVs, which have operated in Monterey Bay, Southern California, the Juan de Fuca plate region offshore of Oregon and Washington states, the Gulf of Mexico, the Gulf of California, and the Lau Basin. The Dorado's are modular, which allows interchanging different sections for specific missions.**

Two examples of research with the CTD/Gulper are chlorophyll peak capture and upwelling front detection and capture. Mapping AUV results presented include location of hydrothermal chimneys, repeat bathymetric surveys, and several surprising discoveries

Keywords—AUV, Autonomous Underwater Vehicle, chlorophyll peak capture, upwelling front detection, sonar mapping, hydrothermal chimneys, repeat bathymetric survey.

I. Dorado Class AUVs

MBARI's Dorado-class AUVs are 53.3 centimeters (21 inches) in diameter and can be as short as 2.4 meters (8 feet) or as long as 6.4 meters (21 feet), depending on the mission. Currently operational Dorado-class AUVs include the upper-water-column vehicle (CTD/Gulper), the seafloor mapping AUV, and the seafloor imaging AUV that incorporates strobe lights and a high-resolution digital camera. The core vehicle elements are rated to 6000 m depth and have been operated up to 20 hours before batteries required recharging.

Fig. 1 CTD/Gulper AUV (left) and Seafloor Mapping AUV (D. Allan B.) on the deck of MBARI's R/V Rachel Carson.

II. Dorado CTD/Gulper AUV (Y.Zhang, J.Harvey, and J.Ryan)

The CTD/Gulper AUV has a suite of physical, chemical, and biological sensors: two Seabird conductivity, temperature, and depth (CTD) sensors, a Satlantic MBARI *in situ* ultraviolet spectrophotometer (ISUS) to monitor nitrate, bromide and bisulfide, a HydroScat-2 optical backscatter and fluorometer (to monitor chlorophyll fluorescence), and a bathyphotometer (pump and photomultiplier tube). It also carries a Sequoia holographic laser *in situ* spectrometer and transmissometer (LISST-Holo: 25 µm to 2.5 mm), a Brooke Ocean Technology laser optical plankton counter (LOPC: 100 µm to 3.5 cm), a LISST-100 (measures from 1.25 µm to 500 µm), and a Seabird SBE 43 dissolved oxygen sensor.

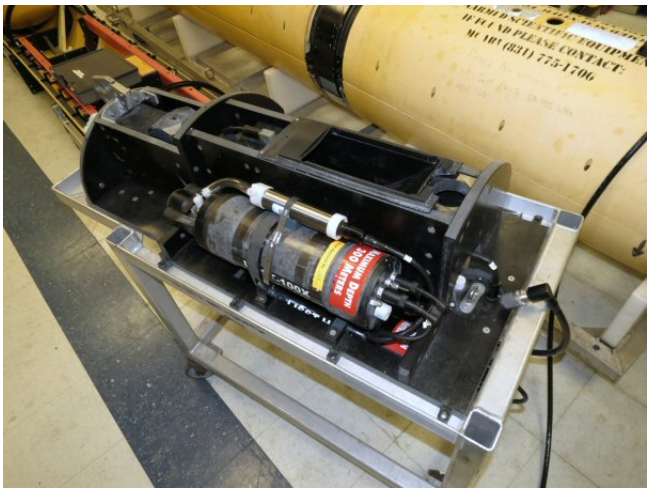

Fig. 2 CTD/Gulper AUV Science Payload (removed from nose of vehicle.)

This AUV also contains an array of ten Gulpers (1.85 L water sampling syringes), triggered by software command (see Fig. 3). [Bird et al. 2007, Thompson 2007].

978-0-933957-40-4 ©2013 MTS

Fig. 3 A single Gulper water sampler with 1.85 L capacity.

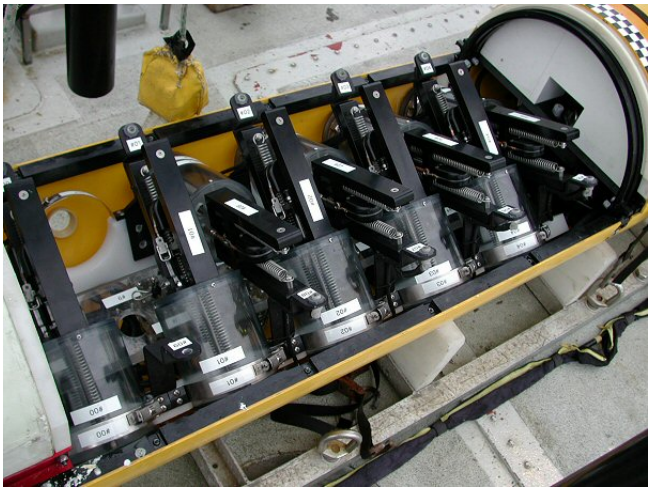

Fig. 4 Gulpers mounted in mid-body section of CTD/Gulper AUV.

The CTD/Gulper AUV combines synoptic environmental data acquisition, high-intake-rate water sampling and real-time signal processing algorithms to enable targeted sampling of oceanographic processes [Ryan et al. 2010, 2013a; Harvey et al. 2012b]. Two prominent examples follow:

A. Example 1-- Chlorophyll signal peak capture in phytoplankton patches:

Phytoplankton patches have important impacts on patterns of primary productivity, the development of harmful algal blooms (HABs), and the survival and growth of zooplankton, including fish and invertebrate larvae. MBARI has developed a peak-capture algorithm for the CTD/Gulper AUV to precisely detect chlorophyll fluorescence peaks and trigger water sample acquisition in phytoplankton patches [Zhang et al. 2010]. In an ascent-descent cycle (see Fig. 5), the vehicle registers the maximum chlorophyll fluorescence signal (using a sliding window) on its first pass through a thin layer. On its second pass through the thin layer, the AUV triggers a gulper as soon as the measured fluorescence reaches the fluorescence peak signal height, recorded on the first pass (in addition to meeting other robustness criteria), thus accurately acquiring a peak-chlorophyll water sample without delay.

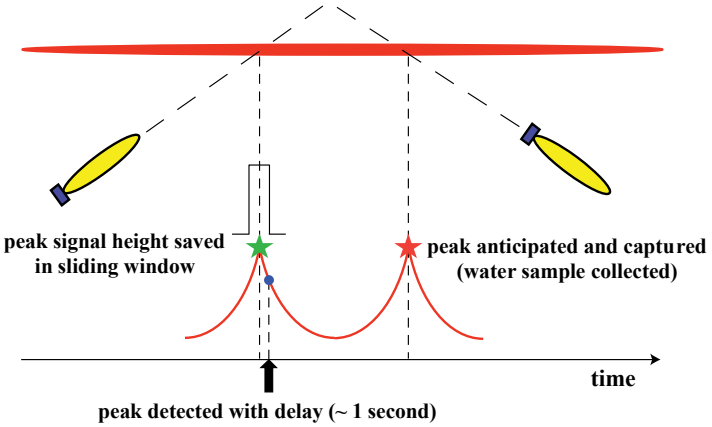

Fig. 5 Graphical representation of the CTD/Gulper AUV employing the chlorophyll peak-capture algorithm to target and capture a water sample. Modified from Zhang et al. 2010.

The chlorophyll peak-capture algorithm cross-checks for concurrent, high optical backscatter signal values to ensure that sampled fluorescence peaks are true biomass maxima. Using sliding temporal windows, the algorithm keeps track of the background levels of chlorophyll fluorescence and optical backscatter signals, as well as the fluorescence signal's average peak level on successive yo-yo profiles, thereby adapting sensitivity to ambient conditions. The AUV peak-capture algorithm has been successfully applied in a series of field programs studying harmful algal blooms (HABs) and zooplankton populations. Application of this method during a patch-tracking study in 2010 revealed small-scale variability in the toxicity of a HAB species and indicated causative processes [Ryan et al. 2013a].

Specifically, in areas where the toxin-producing phytoplankton populations were influenced by resuspended sediments, the phytoplankton were distinctly more toxic (see Fig. 6). The hypothesis for this relationship concerns trace metals, which have been shown in laboratory studies to regulate toxin production in HABs and which may be transported along with sediments.

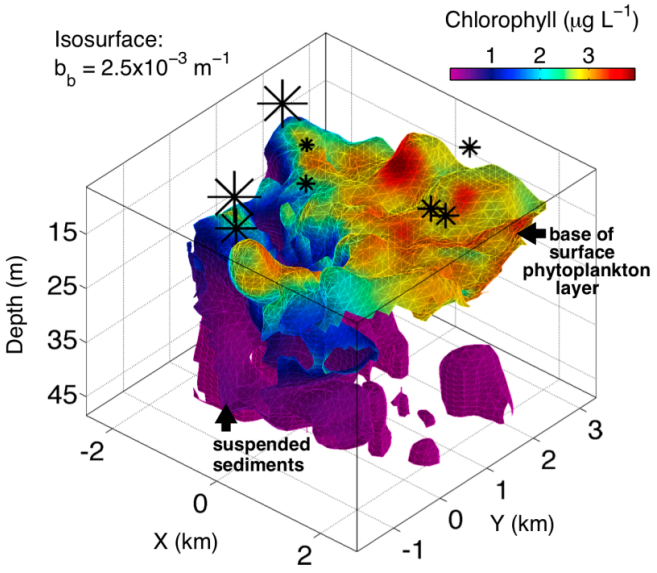

Fig. 6 Quasi-Lagrangian view of the interaction between the surface phytoplankton layer and suspended sediments evidently influencing the toxicity of specific phytoplankton taxa. While phytoplankton are identified in AUV optical data by high chlorophyll fluorescence and optical backscattering (b_b), suspended sediments are identified by low chlorophyll fluorescence and high optical backscattering. This description was derived from intercalibrated measurements by the Dorado and Tethys AUVs within a 46-h period while following a patch tagged by a satellite-tracked drifter. X and Y locations are relative to the drifter. At each sample location, toxin per cell is represented by an asterisk scaled accordingly. From Ryan et al. 2013a.

In an October 2009 experiment in Monterey Bay, California, the AUV triggered water sampling in a phytoplankton patch that was evidently subducted from near-surface waters to near the seafloor in an upwelling front. The water sample contained the highest concentrations of mussel and barnacle larvae detected in the study [Ryan et al. 2013b]. Autonomously locating phytoplankton patches, the AUV sampled this unexpected near-bottom feature. This intelligent sampling, combined with high spatiotemporal resolution of the front in which it was sampled revealed the physical dynamics driving accumulation and transport of larvae.

In April 2013, the AUV ran this algorithm to accurately locate and acquire water samples from subsurface chlorophyll maxima for a HAB study in San Pedro Bay, California, as shown in Fig. 7. Sampling of the phytoplankton populations across two water types (shelf and deep channel) and the front between them enabled examination of species diversity and origins of "seed populations" for blooms of toxin producing species.

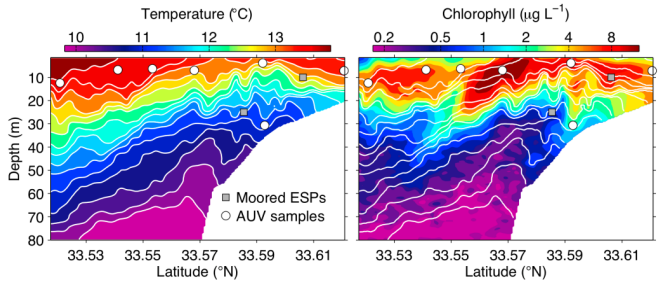

Fig. 7 On 17 March 2013, the Dorado CTD/gulper AUV ran the peak-capture algorithm to acquire water samples (six peak samples plus one off-peak control sample) from subsurface chlorophyll maximum in San Pedro Bay, California.

B. Example 2—Upwelling front detection and sampling:

Nutrients carried up by coastal upwelling fuel primary productivity and support commercially important fisheries. Previous, non-targeted AUV sampling in the Monterey Bay, (see Fig. 9) suggests that zooplankton (e.g., invertebrate larvae and copepods) are aggregated by upwelling fronts and associated with elevated chlorophyll fluorescence [Harvey et al. 2012a].

To investigate complex coastal upwelling ecosystems, we have developed an AUV algorithm to autonomously distinguish between upwelling and stratified water columns and accurately detect the temperature gradient front between them [Zhang et al. 2012] (see Fig. 8).

During June 2011 and May–June 2012 in Monterey Bay, the CTD/Gulper AUV successfully classified three distinct water types: stratified water, upwelling water, and the front in-between (see Fig 8). The AUV also accurately located the narrow front, and acquired targeted water samples from each water type. Molecular analysis of AUV-acquired water samples showed distinct zooplankton signals in the three water types. Novel detection and targeted sampling capabilities thus permit the CTD/gulper AUV to autonomously conduct "surgical sampling" of complex, spatially and temporally variable marine ecosystems.

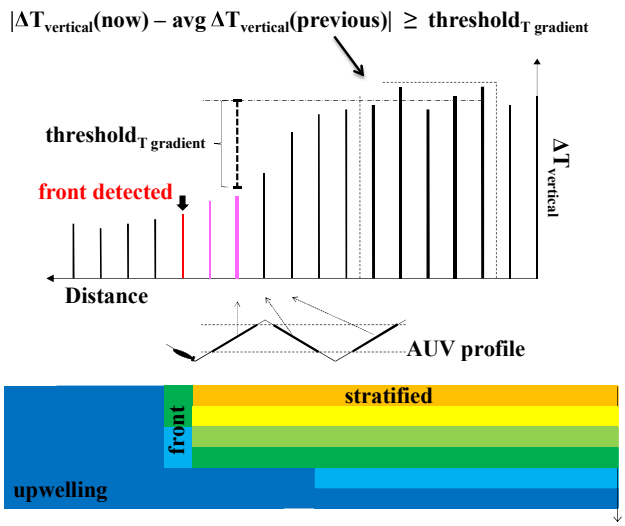

Fig. 8 A graphical representation of the upwelling front sampling algorithm employed by the CTD/Gulper AUV, with corresponding water types indicated below. The AUV accurately locates the front when detecting a sharp horizontal gradient of the vertical temperature difference $\Delta T_{vertical}$, and accordingly triggers water sampling. Modified from Y. Zhang et al. 2012.

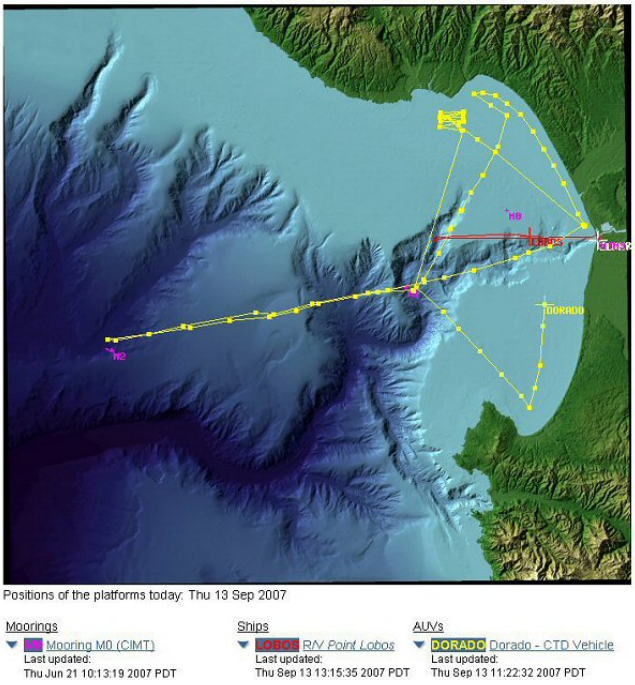

Fig. 9 CTD/Gulper AUV survey mission tracks in Monterey Bay, September 2007, prior to the development of the surgical sampling techniques.

III. MAPPING AUV

The D. Allan B. Mapping AUV is a modularized Dorado Class 54 cm (21 inch) diameter, 5.18 meter (17 feet) length, 733 kg (1616 pounds) air weight. The interior of the AUV floods with water when launched; electronics are contained in either one-atmosphere hermetic housings or in pressure-compensated enclosures. The AUV is ballasted to be about 3.63 kg (8 pounds) positive in seawater. Flotation is accomplished with 6000 meter rated syntactic foam. The D. Allan B. has three mapping sonar systems onboard: a Reson Seabat 7125 200 kHz multibeam echosounder, an Edgetech FS-AU Sonar Package which comprises a 100 kHz chirp sidescan, a 410 kHz chirp sidescan, and a 1-6 kHz chirp subbottom profiler. With the onboard lithium polymer battery packs, the Mapping AUV has an endurance of approximately 17 hours at a speed of 1.5 meters per second, providing a range of 55 to 85 kilometers. The mapping AUV is equipped with a Kearfott inertial navigation system (INS) with Doppler velocity logger, a Paroscientific pressure sensor, and an ultrashort baseline (USBL) transponder and an acoustic modem for communications. It also has an Iridium satellite short burst data modem, a drop weight, radio direction finder, Homer Pro beacon and visible strobe location aids. Propulsion is accomplished with a duct-protected articulated propeller which provides 52 Newtons (12lbf) of thrust at 300 rpm as well as elevator and rudder functions. Turning diameter is less than 20 meters; climb/dive rate is approximately 30 meters per minute.

A. Hydrothermal Chimneys (D. Clague)

The mapping AUV surveys (see Fig. 10) led researchers to identify hydrothermal chimneys and then dive directly on them instead of having to do the usual homing in on water column anomalies using expensive ROV or submersible time. At the Alarcon Rise, because we mapped the region first, our first ROV dive on the ridge using the Doc Rickets reached tall chimneys within 15 minutes of hitting bottom.

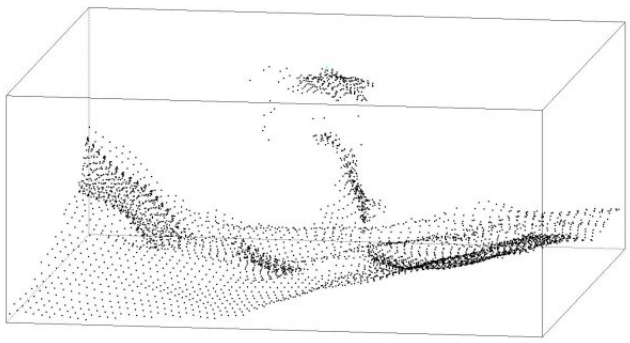

Fig. 10 Point Cloud of Hydrothermal Chimney on the Alarcon Rise, Gulf of California, April 2013.

Prior searches for active chimneys commonly required many dives and a good deal of luck to locate. The chimneys, of course, are of interest to geologists, water chemists, and biologists and have been the focus of an enormous amount of

submersible and ROV work over the last 35 years (see Fig 11).

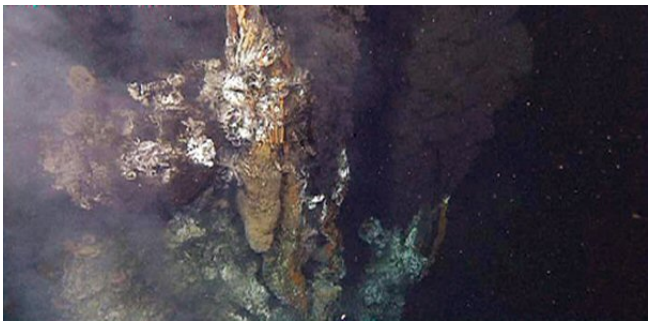

Fig. 11 Hydrothermal Vent on the Alarcon Rise.

Another discovery relates to how deep sea lava flows are constructed--the architecture of the flows. They are commonly combinations of the pillow, lobate, and sheet lavas that have been known for decades, but we now can see that all these lava morphologies are commonly produced during single eruptions and are arranged in specific configurations that reflect the processes of flow emplacement.

Sidescan results allow us to map out young, nearly sediment-free flows from older flows with more sediment cover. This, coupled with the bathymetry that lets us identify flow boundaries, allows us to design ROV dives that can sample the maximum number of flows during single dives rather than driving around on single flows for long periods.

B. Repeat bathymetric surveys (D. Caress)

Technically, our most difficult achievement has been resolving lava flow thickness of the Axial Seamount 2011 eruption using repeat surveys. [Caress, et al., 2012]. The MBARI mapping AUV D. Allan B. surveyed the region before and after the eruption, which enabled MBARI researchers to precisely map the extent, volume, and changing morphology along the length of the flows (see Fig. 13).

In addition to showing in great detail the architecture of the flows (see Fig. 12), this data revealed that the same fissures and channel systems can be reused eruption after eruption, which is intriguing volcanologically but also means that mapping out the boundaries of older, partially buried flows might be more difficult.

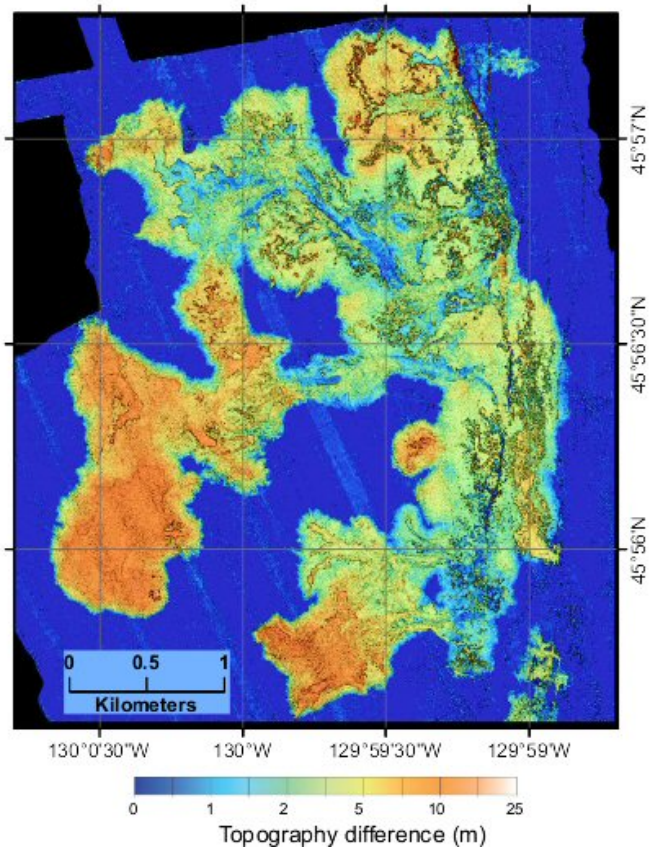

Fig. 12 The volcanic eruption in 2011 at Axial Seamount on the Juan de Fuca mid-ocean ridge produced lava flows that are well-defined in this map of the difference between pre- and post-eruption AUV bathymetry. The eruption reused pre-existing fissures and channels, flooded across large areas as sheet flows, and at the distal ends transitioned to inflated lobate flows 10-15 m thick [Caress et al., 2012].

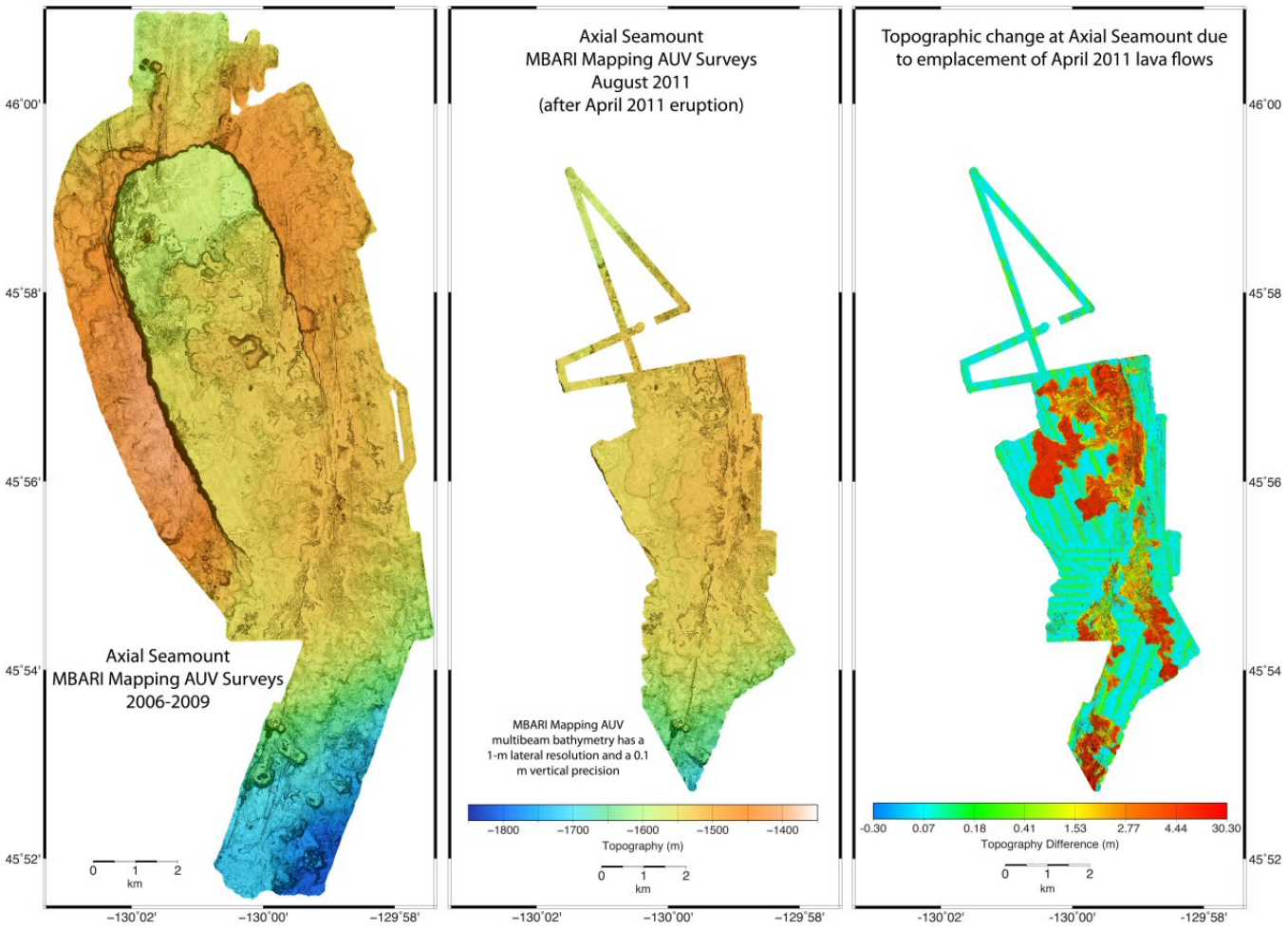

Fig. 13 Repeat Bathymetric Survey on the Axial Seamount. (Left pane) Initial Axial Seamount Surveys 2006-2009, (middle) Post-Eruption Survey 2011, (right) map of topographic change due to lava flow.

C. Davidson Seamount lava flows (J. Paduan)

A surprising result is the ponded and collapsed lava flow (see Fig. 14) at Davidson Seamount that were observed in the AUV map and then dove on with the ROV (see Fig. 16).

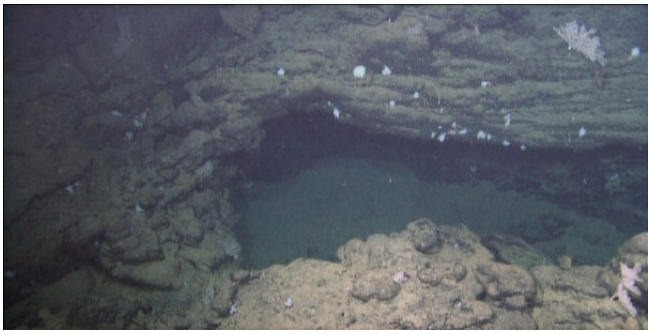

Fig. 14 Collapsed lava flow on Davidson Seamount.

Such a feature is unusual on the seamounts off California, which are otherwise composed of blocky or pillow flows (see Fig. 15.)

Fig. 15 Pillow lava flow on the Davidson Seamount.

The ponded and collapsed lava flow was not visible in the lower-resolution ship-based bathymetry but was clear in the AUV data, and is an example of how one can't assume everything is known about a seamount from low-resolution maps or a few submersible dives.

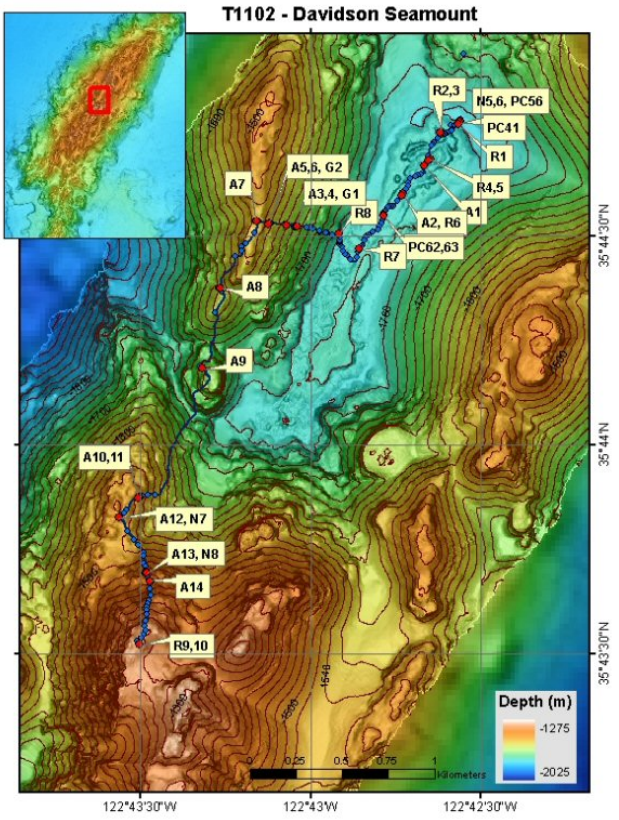

Fig. 16 Dive map of the Davidson Seamount.

D. Surprise Discoveries (C. Paull)

The mapping AUV has been used to conduct ~40 surveys along the continental margin of western North America. These have focused on mapping within submarine canyons and around submarine gas venting sites. Unexpected results include the realization that crescent-shaped bed forms (Paull et al., 2011) are common within the submarine canyons along the coast of California (see Fig. 17); the size of the deep-water bed forms seen on canyon floors (see Fig. 18); and the distinctive shapes of gas venting features (see Fig. 19).

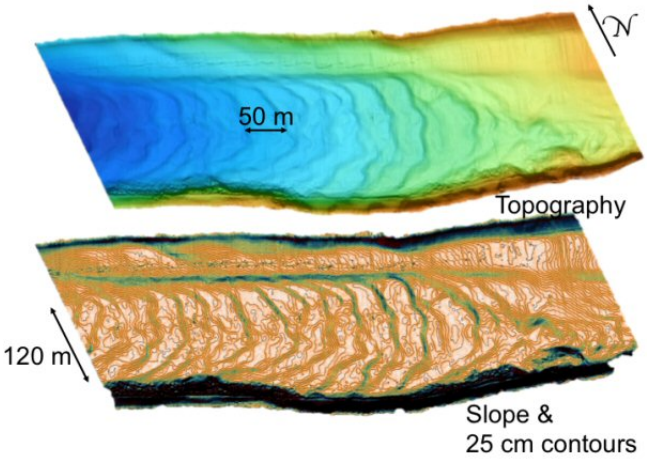

Fig. 17 Images showing crescent-shaped bed forms within the axial channel of upper Monterey Canyon between 273 and 303 m water depths. Above is a perspective view of the topography while below the same area is shown at a 25 cm contour interval shaded by slope.

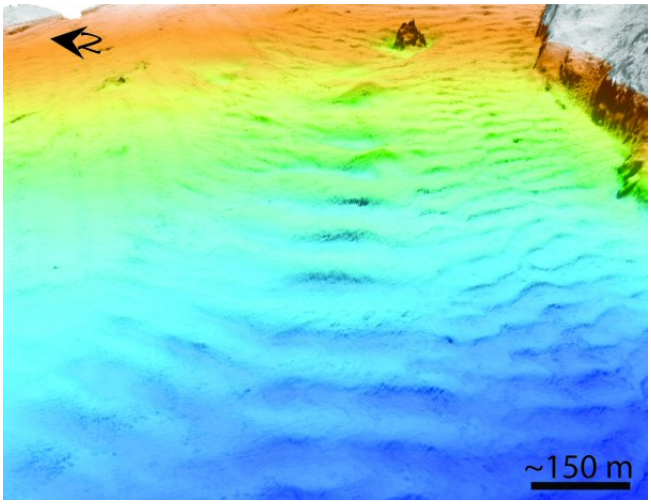

Fig. 18 Image shows large bedforms on the floor of Monterey Canyon in 1860 to 1810 water depths.

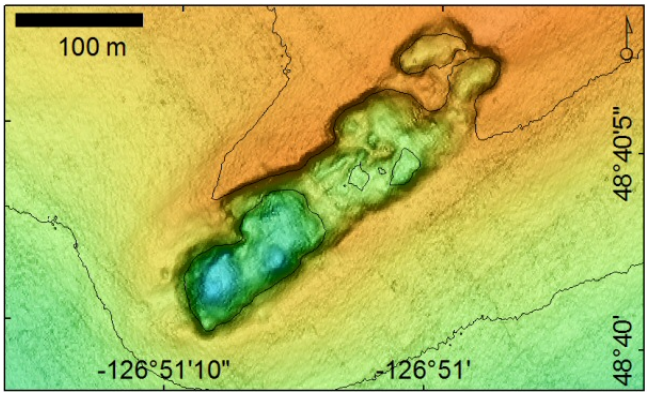

Fig. 19 Image of the topography of Bullseye Vent off British Columbia, which reveals this feature is associated with a ~350 m long and up to 5 m deep depression.

ACKNOWLEDGMENT

MBARI is a non-profit research center funded by The David and Lucile Packard Foundation. R. McEwen and J. Bellingham contributed to the development of the Dorado AUV's phytoplankton patch sampling and upwelling front sampling algorithms.

REFERENCES

Bird, L. E., A. Sherman, and J. Ryan (2007), "Development of an active, large volume, discrete seawater sampler for autonomous underwater vehicles," in *Proceedings of MTS/IEEE OCEANS'07 Conference*, pp. 1-5, Vancouver, BC, Canada.

Harvey, J. B. J., J. P. Ryan, R. Marin III, C. M. Preston, N. Alvarado, C. A. Scholin, R. C. Vrijenhoek (2012a), "Robotic sampling, in situ monitoring and molecular detection of marine zooplankton," *Journal of Experimental Marine Biology and Ecology*, Vol. 413, pp. 60–70.

Harvey, J. B. J., Y. Zhang, and J. P. Ryan (2012b), "AUVs for Ecological Studies of Marine Plankton Communities - Intelligent Algorithms on Dorado and Tethys AUVs Enable Precise Water Sampling for Plankton Research," *Sea Technology*, Vol. 53, No. 9, pp. 51-54.

Paull, C.K., D. Caress, W. Ussler III, E. Lundsten, and M.C. Meiner-Johnson, (2011), "*High-resolution bathymetry of the axial channels within Monterey and Soquel submarine canyons; offshore central California*, Geospheres," Vol. 7, pp. 1-26.

Ryan, J.P., S. B. Johnson, A. Sherman, K. Rajan, F. Py, H. Thomas, J. B. J. Harvey, L. Bird, J. D. Paduan, and R. C. Vrijenhoek (2010), "Mobile autonomous process sampling within coastal ocean observing systems," *Limnology and Oceanography: Methods*, Vol. 8, pp. 394–402.

Ryan, J. P., et al. (2013), "Boundary influences on HAB phytoplankton ecology in a stratification-enhanced upwelling shadow," *Deep Sea Research II*, in press.

Ryan, J. P., J. B. J. Harvey, Y. Zhang, and C. B. Woodson (2013), "Small-scale processes of larval accumulation and transport in an upwelling shadow", in preparation.

Thompson, D. R. (2007), "AUV operations at MBARI," in *Proceedings of MTS/IEEE OCEANS'07 Conference*, Vancouver, BC, Canada, pp. 1-6.

Zhang, Y., R. S. McEwen, J. P. Ryan, and J. G. Bellingham (2010), "Design and Tests of an Adaptive Triggering Method for Capturing Peak Samples in a Thin Phytoplankton Layer by an Autonomous Underwater Vehicle," *IEEE Journal of Oceanic Engineering*, Vol. 35, No. 4, pp. 785-796.

Zhang, Y., J. P. Ryan, J. G. Bellingham, J. B. J. Harvey, and R. S. McEwen (2012), "Autonomous detection and sampling of water types and fronts in a coastal upwelling system by an autonomous underwater vehicle," *Limnology and Oceanography: Methods*, Vol. 10, pp. 934-951.